

Measurement of the Average Polarization of b Baryons in Hadronic Z⁰ Decays

The OPAL Collaboration

Abstract

In the Standard Model, b quarks produced in e⁺e⁻ annihilation at the Z⁰ peak have a large average longitudinal polarization of -0.94. Some fraction of this polarization is expected to be transferred to b-flavored baryons during hadronization. The average longitudinal polarization of weakly decaying b baryons, $\langle P_L^{\Lambda_b} \rangle$, is measured in approximately 4.3 million hadronic Z⁰ decays collected with the OPAL detector between 1990 and 1995 at LEP. Those b baryons that decay semileptonically and produce a Λ baryon are identified through the correlation of the baryon number of the Λ and the electric charge of the lepton. In this semileptonic decay, the ratio of the neutrino energy to the lepton energy is a sensitive polarization observable. The neutrino energy is estimated using missing energy measurements. From a fit to the distribution of this ratio, the value

$$\langle P_L^{\Lambda_b} \rangle = -0.56_{-0.13}^{+0.20} \pm 0.09$$

is obtained, where the first error is statistical and the second systematic.

Submitted to *Physics Letters B*

The OPAL Collaboration

G. Abbiendi², K. Ackerstaff⁸, G. Alexander²³, J. Allison¹⁶, N. Altekamp⁵, K.J. Anderson⁹, S. Anderson¹², S. Arcelli¹⁷, S. Asai²⁴, S.F. Ashby¹, D. Axen²⁹, G. Azuelos^{18,a}, A.H. Ball¹⁷, E. Barberio⁸, R.J. Barlow¹⁶, R. Bartoldus³, J.R. Batley⁵, S. Baumann³, J. Bechtluft¹⁴, T. Behnke²⁷, K.W. Bell²⁰, G. Bella²³, A. Bellerive⁹, S. Bentvelsen⁸, S. Bethke¹⁴, S. Betts¹⁵, O. Biebel¹⁴, A. Biguzzi⁵, S.D. Bird¹⁶, V. Blobel²⁷, I.J. Bloodworth¹, M. Bobinski¹⁰, P. Bock¹¹, J. Böhme¹⁴, D. Bonacorsi², M. Boutemour³⁴, S. Braibant⁸, P. Bright-Thomas¹, L. Brigliadori², R.M. Brown²⁰, H.J. Burckhart⁸, C. Burgard⁸, R. Bürgin¹⁰, P. Capiluppi², R.K. Carnegie⁶, A.A. Carter¹³, J.R. Carter⁵, C.Y. Chang¹⁷, D.G. Charlton^{1,b}, D. Chrisman⁴, C. Ciocca², P.E.L. Clarke¹⁵, E. Clay¹⁵, I. Cohen²³, J.E. Conboy¹⁵, O.C. Cooke⁸, C. Couyoumtzelis¹³, R.L. Coxe⁹, M. Cuffiani², S. Dado²², G.M. Dallavalle², R. Davis³⁰, S. De Jong¹², L.A. del Pozo⁴, A. de Roeck⁸, K. Desch⁸, B. Dienes^{33,d}, M.S. Dixit⁷, J. Dubbert³⁴, E. Duchovni²⁶, G. Duckeck³⁴, I.P. Duerdoth¹⁶, D. Eatough¹⁶, P.G. Estabrooks⁶, E. Etzion²³, H.G. Evans⁹, F. Fabbri², M. Fanti², A.A. Faust³⁰, F. Fiedler²⁷, M. Fierro², I. Fleck⁸, R. Folman²⁶, A. Fürties⁸, D.I. Futyan¹⁶, P. Gagnon⁷, J.W. Gary⁴, J. Gascon¹⁸, S.M. Gascon-Shotkin¹⁷, G. Gaycken²⁷, C. Geich-Gimbel³, G. Giacomelli², P. Giacomelli², V. Gibson⁵, W.R. Gibson¹³, D.M. Gingrich^{30,a}, D. Glenzinski⁹, J. Goldberg²², W. Gorn⁴, C. Grandi², E. Gross²⁶, J. Grunhaus²³, M. Gruwe²⁷, G.G. Hanson¹², M. Hansroul⁸, M. Hapke¹³, K. Harder²⁷, C.K. Hargrove⁷, C. Hartmann³, M. Hauschild⁸, C.M. Hawkes⁵, R. Hawkings²⁷, R.J. Hemingway⁶, M. Herndon¹⁷, G. Herten¹⁰, R.D. Heuer⁸, M.D. Hildreth⁸, J.C. Hill⁵, S.J. Hillier¹, P.R. Hobson²⁵, A. Hocker⁹, R.J. Homer¹, A.K. Honma^{28,a}, D. Horváth^{32,c}, K.R. Hossain³⁰, R. Howard²⁹, P. Hütemeyer²⁷, P. Igo-Kemenes¹¹, D.C. Imrie²⁵, K. Ishii²⁴, F.R. Jacob²⁰, A. Jawahery¹⁷, H. Jeremie¹⁸, M. Jimack¹, C.R. Jones⁵, P. Jovanovic¹, T.R. Junk⁶, D. Karlen⁶, V. Kartvelishvili¹⁶, K. Kawagoe²⁴, T. Kawamoto²⁴, P.I. Kayal³⁰, R.K. Keeler²⁸, R.G. Kellogg¹⁷, B.W. Kennedy²⁰, A. Klier²⁶, S. Kluth⁸, T. Kobayashi²⁴, M. Kobel^{3,e}, D.S. Koetke⁶, T.P. Kokott³, M. Kolrep¹⁰, S. Komamiya²⁴, R.V. Kowalewski²⁸, T. Kress¹¹, P. Krieger⁶, J. von Krogh¹¹, T. Kuhl³, P. Kyberd¹³, G.D. Lafferty¹⁶, D. Lanske¹⁴, J. Lauber¹⁵, S.R. Lautenschlager³¹, I. Lawson²⁸, J.G. Layter⁴, D. Lazic²², A.M. Lee³¹, D. Lellouch²⁶, J. Letts¹², L. Levinson²⁶, R. Liebisch¹¹, B. List⁸, C. Littlewood⁵, A.W. Lloyd¹, S.L. Lloyd¹³, F.K. Loebinger¹⁶, G.D. Long²⁸, M.J. Losty⁷, J. Ludwig¹⁰, D. Liu¹², A. Macchiolo², A. Macpherson³⁰, W. Mader³, M. Mannelli⁸, S. Marcellini², C. Markopoulos¹³, A.J. Martin¹³, J.P. Martin¹⁸, G. Martinez¹⁷, T. Mashimo²⁴, P. Mättig²⁶, W.J. McDonald³⁰, J. McKenna²⁹, E.A. Mckigney¹⁵, T.J. McMahon¹, R.A. McPherson²⁸, F. Meijers⁸, S. Menke³, F.S. Merritt⁹, H. Mes⁷, J. Meyer²⁷, A. Michelini², S. Mihara²⁴, G. Mikenberg²⁶, D.J. Miller¹⁵, R. Mir²⁶, W. Mohr¹⁰, A. Montanari², T. Mori²⁴, K. Nagai⁸, I. Nakamura²⁴, H.A. Neal¹², B. Nellen³, R. Nisius⁸, S.W. O'Neale¹, F.G. Oakham⁷, F. Odorici², H.O. Ogren¹², M.J. Oreglia⁹, S. Orito²⁴, J. Pálincás^{33,d}, G. Pásztor³², J.R. Pater¹⁶, G.N. Patrick²⁰, J. Patt¹⁰, R. Perez-Ochoa⁸, S. Petzold²⁷, P. Pfeifenschneider¹⁴, J.E. Pilcher⁹, J. Pinfold³⁰, D.E. Plane⁸, P. Poffenberger²⁸, J. Polok⁸, M. Przybycień⁸, C. Rembser⁸, H. Rick⁸, S. Robertson²⁸, S.A. Robins²², N. Rodning³⁰, J.M. Roney²⁸, K. Roscoe¹⁶, A.M. Rossi², Y. Rozen²², K. Runge¹⁰, O. Runolfsson⁸, D.R. Rust¹², K. Sachs¹⁰, T. Saeki²⁴, O. Sahr³⁴, W.M. Sang²⁵, E.K.G. Sarkisyan²³, C. Sbarra²⁹, A.D. Schaile³⁴, O. Schaile³⁴, F. Scharf³, P. Scharff-Hansen⁸, J. Schieck¹¹, B. Schmitt⁸, S. Schmitt¹¹, A. Schöning⁸, M. Schröder⁸, M. Schumacher³, C. Schwick⁸, W.G. Scott²⁰, R. Seuster¹⁴, T.G. Shears⁸, B.C. Shen⁴, C.H. Shepherd-Themistocleous⁸, P. Sherwood¹⁵, G.P. Siroli², A. Sittler²⁷, A. Skuja¹⁷, A.M. Smith⁸, G.A. Snow¹⁷, R. Sobie²⁸, S. Söldner-Rembold¹⁰, M. Sproston²⁰, A. Stahl³, K. Stephens¹⁶, J. Steuerer²⁷, K. Stoll¹⁰, D. Strom¹⁹, R. Ströhmer³⁴, B. Surrow⁸, S.D. Talbot¹, S. Tanaka²⁴, P. Taras¹⁸, S. Tarem²², R. Teuscher⁸, M. Thiergen¹⁰, M.A. Thomson⁸, E. von Törne³, E. Torrence⁸, S. Towers⁶, I. Trigger¹⁸, Z. Trócsányi³³, E. Tsur²³, A.S. Turcot⁹, M.F. Turner-Watson⁸, R. Van Kooten¹², P. Vannerem¹⁰, M. Verzocchi¹⁰, H. Voss³, F. Wäckerle¹⁰, A. Wagner²⁷, C.P. Ward⁵, D.R. Ward⁵, P.M. Watkins¹, A.T. Watson¹, N.K. Watson¹, P.S. Wells⁸, N. Wermes³, J.S. White⁶,

G.W. Wilson¹⁶, J.A. Wilson¹, T.R. Wyatt¹⁶, S. Yamashita²⁴, G. Yekutieli²⁶, V. Zacek¹⁸, D. Zer-Zion⁸

- ¹School of Physics and Astronomy, University of Birmingham, Birmingham B15 2TT, UK
²Dipartimento di Fisica dell' Università di Bologna and INFN, I-40126 Bologna, Italy
³Physikalisches Institut, Universität Bonn, D-53115 Bonn, Germany
⁴Department of Physics, University of California, Riverside CA 92521, USA
⁵Cavendish Laboratory, Cambridge CB3 0HE, UK
⁶Ottawa-Carleton Institute for Physics, Department of Physics, Carleton University, Ottawa, Ontario K1S 5B6, Canada
⁷Centre for Research in Particle Physics, Carleton University, Ottawa, Ontario K1S 5B6, Canada
⁸CERN, European Organisation for Particle Physics, CH-1211 Geneva 23, Switzerland
⁹Enrico Fermi Institute and Department of Physics, University of Chicago, Chicago IL 60637, USA
¹⁰Fakultät für Physik, Albert Ludwigs Universität, D-79104 Freiburg, Germany
¹¹Physikalisches Institut, Universität Heidelberg, D-69120 Heidelberg, Germany
¹²Indiana University, Department of Physics, Swain Hall West 117, Bloomington IN 47405, USA
¹³Queen Mary and Westfield College, University of London, London E1 4NS, UK
¹⁴Technische Hochschule Aachen, III Physikalisches Institut, Sommerfeldstrasse 26-28, D-52056 Aachen, Germany
¹⁵University College London, London WC1E 6BT, UK
¹⁶Department of Physics, Schuster Laboratory, The University, Manchester M13 9PL, UK
¹⁷Department of Physics, University of Maryland, College Park, MD 20742, USA
¹⁸Laboratoire de Physique Nucléaire, Université de Montréal, Montréal, Quebec H3C 3J7, Canada
¹⁹University of Oregon, Department of Physics, Eugene OR 97403, USA
²⁰CLRC Rutherford Appleton Laboratory, Chilton, Didcot, Oxfordshire OX11 0QX, UK
²²Department of Physics, Technion-Israel Institute of Technology, Haifa 32000, Israel
²³Department of Physics and Astronomy, Tel Aviv University, Tel Aviv 69978, Israel
²⁴International Centre for Elementary Particle Physics and Department of Physics, University of Tokyo, Tokyo 113, and Kobe University, Kobe 657, Japan
²⁵Institute of Physical and Environmental Sciences, Brunel University, Uxbridge, Middlesex UB8 3PH, UK
²⁶Particle Physics Department, Weizmann Institute of Science, Rehovot 76100, Israel
²⁷Universität Hamburg/DESY, II Institut für Experimental Physik, Notkestrasse 85, D-22607 Hamburg, Germany
²⁸University of Victoria, Department of Physics, P O Box 3055, Victoria BC V8W 3P6, Canada
²⁹University of British Columbia, Department of Physics, Vancouver BC V6T 1Z1, Canada
³⁰University of Alberta, Department of Physics, Edmonton AB T6G 2J1, Canada
³¹Duke University, Dept of Physics, Durham, NC 27708-0305, USA
³²Research Institute for Particle and Nuclear Physics, H-1525 Budapest, P O Box 49, Hungary
³³Institute of Nuclear Research, H-4001 Debrecen, P O Box 51, Hungary
³⁴Ludwigs-Maximilians-Universität München, Sektion Physik, Am Coulombwall 1, D-85748 Garching, Germany

^a and at TRIUMF, Vancouver, Canada V6T 2A3

^b and Royal Society University Research Fellow

^c and Institute of Nuclear Research, Debrecen, Hungary

^d and Department of Experimental Physics, Lajos Kossuth University, Debrecen, Hungary

^e on leave of absence from the University of Freiburg

1 Introduction

According to the Standard Model, the process $e^+e^- \rightarrow Z^0 \rightarrow b\bar{b}$ gives rise to b quarks that are longitudinally polarized [1, 2] with a large average value of $\langle P_L^b \rangle = -0.94$ for a weak mixing angle of $\sin^2 \theta_W = 0.23$. This polarization varies by only $\pm 2\%$ over the full range of the production angle¹ θ . If subsequent hadronization to a Λ_b^0 baryon is considered for example, the light u and d quarks form a spin-0 system and the spin of the Λ_b^0 should be carried entirely by the b quark. In the heavy-quark limit, an important prediction of Heavy Quark Effective Theory (HQET) is that the degrees of freedom of the b quark are decoupled from the spin-0 light diquark so that the Λ_b^0 should retain almost 100% of this polarization [2] with only a slight reduction of about 3% due to hard gluon emission during hadronization [3]. This can be contrasted with spin-0 pseudoscalar B mesons where the polarization information of the b quark is lost or vector B^* meson where the polarization information is not expected to be observable [4]. In b baryon production, it is also possible for the b quark to combine with a spin-1 uu , ud , or dd diquark system to form the higher mass baryonic states Σ_b and Σ_b^* that are expected to decay strongly to $\Lambda_b^0\pi$ leading to substantial reduction in the polarization averaged over the weakly decaying b baryons [4, 5]. Measuring the Λ_b polarization² therefore provides a test of HQET and information about heavy baryon hadronization and nonperturbative corrections to spin transfer in fragmentation.

The sign of measured polarization also gives information on the chirality of the b quark coupling to the weak charged current [6], particularly interesting because of recent analyses testing for the presence of sizeable right-handed components in the $b \rightarrow c$ charged current coupling [7]. However, in this case, a polarization values of specific b baryon states would have to be assumed to extract limits on the right-handed component of the charged current and hence the limits would be strongly model dependent.

In the weak semileptonic decay $\Lambda_b \rightarrow X_c \ell^- \bar{\nu}_\ell X$, both the charged lepton and neutrino energy spectrum are sensitive to $\langle P_L^{\Lambda_b} \rangle$ [1, 2, 8]. Assuming that b decays proceed via the usual left-handed current (i.e., $(V - A)$ coupling), in the rest frame of the Λ_b , charged leptons ℓ^- tend to be emitted antiparallel to the spin of the Λ_b and the $\bar{\nu}_\ell$'s parallel to the Λ_b spin. In the laboratory frame, polarization then implies a harder lepton energy spectrum and softer neutrino energy spectrum compared to the unpolarized case. However, there are substantial uncertainties in the exact shape of these spectra due to uncertainties in fragmentation, the ratio of the quark masses m_c/m_b , and QCD corrections [9, 10] such that the extraction of the average polarization from the spectra alone is problematic. These systematic effects partially cancel in the ratio of the average of the lepton energy to the average of the neutrino energy or in the ratios of higher moments of the energy spectra [11, 12].

This paper describes a measurement of the average longitudinal polarization of weakly decaying b baryons, $\langle P_L^{\Lambda_b} \rangle$, using about 4.3 million multihadronic Z^0 decays collected by the OPAL detector from 1990 to 1995. To ensure a data sample with reasonably large statistics, events containing decay chains of the form³ $\Lambda_b \rightarrow \Lambda_c^+ \ell^- \bar{\nu}_\ell X$ followed by $\Lambda_c^+ \rightarrow \Lambda X$ are selected without reconstructing the intermediate charm state. The correlation of a Λ with a negatively-charged lepton ($\ell = e$ or μ) or a $\bar{\Lambda}$ with a positively-charged lepton can indicate the presence of a semileptonic b -baryon decay, as used

¹In the OPAL coordinate system the x axis points towards the center of the LEP ring, the y axis points upwards and the z axis points in the direction of the electron beam. The polar angle θ , the azimuthal angle ϕ and the radius r denote the usual spherical coordinates.

²The symbol Λ_b will be used in this paper to refer to all b baryons that decay weakly, including for example the Λ_b^0 and the b quark in combination with a spin-1 us or ds diquark forming a Ξ_b . The symbol Λ_b^0 is used to denote the particular ground state b baryon with quark content (bud).

³Charge conjugate processes are implied throughout this paper.

previously by OPAL [13, 14]. The other charge combinations ($\bar{\Lambda}\ell^-$ and $\Lambda\ell^+$) are used to characterize the background. The neutrino energy E_ν was estimated using missing energy measurements in the hemisphere containing the $\Lambda\ell^-$ pair. To extract the polarization of the b baryon, a fit was then made to the distribution of the ratio E_ν/E_ℓ formed event by event. Fitting to the shape of this distribution should lead to an estimate with lower statistical variance than the use of the average sample energies $\langle E_\nu \rangle / \langle E_\ell \rangle$ as employed in the previously published measurement of $\langle P_L^{\Lambda b} \rangle$ [15].

2 The OPAL detector

A detailed description of the OPAL detector can be found elsewhere [16]. The almost complete hermeticity of the OPAL detector allows the missing energy in an event to be determined effectively. The central tracking detector consists of a two-layer silicon microstrip detector with polar angle coverage $|\cos\theta| < 0.8$ immediately surrounding the beam-pipe, followed by a high-precision vertex drift chamber, a large-volume jet chamber that records the momentum and energy loss of charged particles over 98% of the solid angle, and chambers which measure the z -coordinate, all in a uniform 0.435 T axial magnetic field. Charged particles can be identified by their specific ionization energy loss, dE/dx , in the jet chamber. Further information on the performance of the tracking and dE/dx measurements can be found in Ref. [17]. A lead-glass electromagnetic calorimeter is located outside the magnet coil, which, in combination with the forward calorimeter, gamma catcher and silicon-tungsten luminometer [18], complete the geometrical acceptance down to 24 mrad from the beam direction. The magnet return yoke is instrumented with streamer tubes for hadron calorimetry and is surrounded by several layers of muon chambers.

3 Monte Carlo simulations

To model the signal, samples of simulated data were generated of Z^0 hadronic decays that included $\Lambda_b^0 \rightarrow \Lambda_c^+ \ell^- \bar{\nu}_\ell X$ followed by $\Lambda_c^+ \rightarrow \Lambda \pi^+ X$ and $\Lambda \rightarrow p \pi^-$ using a modified JETSET decay routine incorporating polarized Λ_b^0 decay with QCD corrections as described in Ref. [10]. Samples of 40 000 events each were generated at twelve different values of $\langle P_L^{\Lambda b} \rangle$. These signal samples and the heavy flavor Monte Carlo event samples described below were generated using the latest world average branching ratios for Λ_c decays [19]. Additional samples including primary production and decay of Σ_b or Ξ_b baryons were used to assess the effect of the presence of different baryons on the result.

Monte Carlo simulation samples of inclusive hadronic Z^0 decays were used to check backgrounds. The JETSET 7.4 parton shower Monte Carlo generator [20] with the fragmentation function of Peterson *et al.* [21] for heavy quarks was used to generate samples including approximately 4 million hadronic Z^0 decays and 2 million $Z^0 \rightarrow b\bar{b}$ decays (the equivalent of about 9 million hadronic decays). As will be discussed later, in the decay $b \rightarrow \tau \bar{\nu}_\tau X$ when the τ decays leptonically, the resulting lepton and neutrino background has to be taken into account carefully. The tau polarization in these decays was calculated according to Ref. [22] and leptonic decays of these and all other τ leptons were handled by the TAUOLA package [23].

All Monte Carlo samples were processed through a full simulation of the OPAL detector [24] and the same event analysis chain was applied to the simulated events as to the data.

4 Data and event selection

This analysis uses data collected at center-of-mass energies within ± 3 GeV of the Z^0 mass during the 1990–1995 LEP running periods. Following detector performance requirements, track quality cuts, and a standard hadronic event selection [25], a data sample of 4.3 million multihadronic events was selected. Given the importance of having well contained events in the detector for a reliable measurement of the missing energy, each event was required to have $|\cos \theta_{\text{thr}}| < 0.85$ where θ_{thr} is the polar angle of the thrust axis.

The selection of b-baryon decays using Λ -lepton pairs is similar to the one previously used to measure the average b-baryon lifetime and production rate [14] but uses improved electron identification, a different jet definition, different lepton kinematic cuts, and the inclusion of an additional π^+ to exploit the charge correlation of Λ - π^+ in the decay chain $\Lambda_b \rightarrow \Lambda_c^+ \rightarrow \Lambda \pi^+ X$. These all contribute to an overall improvement of the signal-to-purity ratio by 45%. Firstly, electrons and muons having large momentum and large transverse momentum with respect to their associated jet (including the lepton candidate) were identified. Λ baryons were then reconstructed and combined with π^+ 's that were consistent with coming from a common vertex formed by the Λ and lepton candidate. In the signal process the π^+ most commonly comes from the Λ_c^+ decay with a decay length from the point of Λ_b decay which is small compared with the typical Λ -lepton vertex resolution. Requirements were placed on the Λ -lepton combination followed by requirements to improve the missing energy determination and its applicability in estimating the neutrino energy in the semileptonic decay of the Λ_b .

Electrons were identified using an artificial neural network which is a simplified version of that described in Ref. [26], using only six rather than twelve inputs. These are: the momentum and polar angle of the track, the energy-momentum ratio E/p , the number of electromagnetic calorimeter blocks contributing to the energy measurement, the ionization energy loss and its error. Photon conversion candidates were rejected using another neural network algorithm, similar to that described in Ref. [26], but using the new electron identification algorithm to identify the conversion partner to the electron candidate. Muon candidates were identified by associating track segments in the outer muon detectors with tracks extrapolated from the central tracking detectors [27].

Charged tracks and electromagnetic clusters not associated with charged tracks were combined into jets using a cone algorithm [28] with a minimum jet energy of 5.0 GeV and cone half angle of 550 mrad. Electron and muon candidates were required to have momentum greater than 4.0 GeV and transverse momentum with respect to the associated jet axis, p_t , greater than 0.7 GeV to obtain a sample enriched in b-quark events.

Candidate Λ baryons decaying via $\Lambda \rightarrow p\pi^-$ were identified as described in Ref. [14] by considering oppositely charged tracks assigned to the same jet as the lepton and satisfying dE/dx criteria and various kinematic and geometric requirements. To reduce $K_S^0 \rightarrow \pi^+\pi^-$ contamination, the invariant mass, measured assuming a pion mass for both particles, was required to be more than one standard deviation in mass resolution away from the K_S^0 mass: less than 0.491 GeV or greater than 0.503 GeV. To decrease the contribution of Λ candidates coming from fragmentation processes, the Λ candidate was required to have a minimum momentum of 4 GeV. The invariant mass of the reconstructed Λ was required to be between 1.1078 and 1.1234 GeV. The fraction of Λ baryons wrongly identified as $\bar{\Lambda}$ is negligible since for these Λ momenta the proton candidate can always be taken as the higher momentum track. The efficiency of this selection varies from 23% to 10% for low to high momentum Λ candidates.

Lepton and Λ candidates were then correlated using the following criteria. The reconstructed momentum vector of the Λ candidate was required to be closer than 50° to the momentum vector of the lepton candidate. The invariant mass of the Λ -lepton system was demanded to be greater than 2.2 GeV to reduce the background from Λ_c^+ 's that decay semileptonically: $\Lambda_c^+ \rightarrow \Lambda \ell^+ \nu_\ell$. To reduce further random combinatorial background, the magnitude of the momentum vector sum of the Λ and lepton had to be greater than 9 GeV.

For each accepted Λ -lepton pair, candidate π^+ 's were selected among all charged tracks in the jet to which the lepton was assigned. Charged tracks with momentum greater than 0.5 GeV and with measured dE/dx having a probability greater than 1% of being consistent with a pion were considered for combining in the vertex. The track was required to be positively charged if combined with a Λ , and negatively charged if combined with a $\bar{\Lambda}$. A decay vertex was formed in the r - ϕ plane by extrapolating the candidate Λ momentum vector from its decay vertex to the intersection with the lepton candidate track. The π candidate was then also fitted to the Λ -lepton decay vertex and the candidate track with the largest corresponding χ^2 vertex probability was chosen. $\Lambda \ell^- \pi^+$ combinations were retained if the χ^2 probability of the common fit vertex was greater than 1% and the invariant mass of the common vertex less than 5.6 GeV.

Even for properly reconstructed $\Lambda \ell$ combinations coming from the decay $\Lambda_b \rightarrow \Lambda_c^+ \ell^- \bar{\nu}_\ell$, the subsequent semileptonic decay of $\Lambda_c^+ \rightarrow \Lambda \ell^+ \nu_\ell$ would result in a second neutrino compromising the measurement of E_ν from the Λ_b decay using the missing energy in the event. Therefore a small fraction of the $\Lambda \ell$ combinations were rejected if the π^+ candidate track selected above had momentum greater than 2.0 GeV and was identified as an electron or muon.

Each event was divided into two hemispheres by a plane perpendicular to the thrust axis. The hemisphere containing the $\Lambda \ell^- \pi^+$ combination was defined as the signal hemisphere and the opposite hemisphere as the recoil hemisphere. To reject events with incorrectly measured total energy and therefore fake missing energy due to mismeasurement of momenta, signal hemispheres were rejected if they contained high-momentum tracks close to anode planes in the jet chamber, i.e., with measured momenta greater than 10 GeV and satisfying $|\phi - \phi_{\text{anode}}| < 1^\circ$ where ϕ is the azimuthal angle of the track and ϕ_{anode} is the angle of the closest anode wire plane in the jet chamber. In the hemisphere opposite to the signal hemisphere, additional missing energy can arise due to semileptonic decays of b and c hadrons into electrons and muons. Signal hemispheres were rejected if the opposite hemisphere contained an electron or muon satisfying the kinematic cuts described earlier since the presence of a lepton can indicate the possible presence of a neutrino with substantial energy in the opposite hemisphere from a semileptonic decay.

The invariant mass distribution of the $p\pi^-$ combination is shown in Fig. 1 for $\Lambda \ell^- \pi^+$ (right-sign) and $\Lambda \ell^+ \pi^+$ (wrong-sign) combinations after all other selection requirements have been applied. A total of 912 right-sign and 316 wrong-sign $\Lambda \ell^- \pi^+$ combinations are selected with an overall b baryon purity of 69% in the right-sign sample. The 596 excess right-sign combinations can be attributed mainly to b -baryon decays. The overall efficiency to select true Λ 's and leptons from b baryon semileptonic decays is estimated from Monte Carlo simulated samples to be approximately 5.6%, although a knowledge of this efficiency is not necessary for the polarization measurement. The number of observed wrong-sign combinations will be used after small corrections as an estimate of the level of the background as well as to estimate the shape of the background in the distribution of the ratio E_ν/E_ℓ .

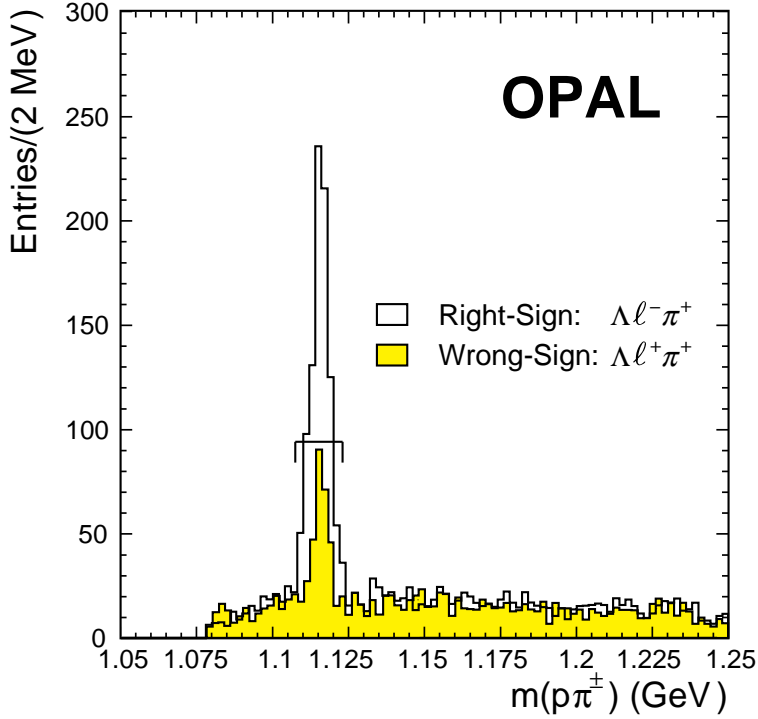


Figure 1: *Invariant mass distribution of $\rho\pi^-$ combinations in the right-sign $\Lambda\ell^-\pi^+$ sample (open histogram) superimposed by wrong-sign $\Lambda\ell^+\pi^+$ (shaded histogram) combinations. Charge conjugate states are implied if not stated otherwise. The signal region is shown by the bracketed range of masses. The peak at the Λ mass in the wrong-sign distribution is indicative of genuine Λ particles (though not necessarily from b -baryon decay, e.g. from fragmentation) being combined with real or fake leptons (i.e., hadrons misidentified as leptons).*

5 Neutrino and lepton energy measurement

In the semileptonic decay of the Λ_b , the neutrino energy was estimated by the measured missing energy in the signal hemisphere, which can be defined by

$$E_\nu = E_{\text{miss}}^{\text{hemi}} = E_{\text{beam}} + E_{\text{corr}} - E_{\text{vis}}^{\text{hemi}},$$

where E_{beam} is the beam energy and $E_{\text{vis}}^{\text{hemi}}$ the visible energy in the signal hemisphere. If we assume a two-body decay of the Z^0 , with each hemisphere considered as one body, then E_{corr} is a correction term calculated assuming that the two hemisphere momenta are equal:

$$E_{\text{corr}} = (M_{\text{sig}}^2 - M_{\text{recoil}}^2)/4E_{\text{beam}}.$$

M_{sig} and M_{recoil} are the measured invariant masses of the signal hemisphere and opposite recoil hemisphere, respectively. The term E_{corr} uses the beam energy constraint to improve the resolution for the missing energy in the signal hemisphere by accounting for fluctuations of energy splitting between hemispheres and unobserved neutral energy on an event by event basis.

Calculations of these quantities used the four-momenta of reconstructed charged tracks and of clusters in the electromagnetic and hadronic calorimeters not associated with charged tracks. The

masses of all charged particles were set to the charged pion mass except for the proton from the identified Λ and the identified lepton which are set to their appropriate masses. The invariant masses of the calorimeter energy clusters were assumed to be zero. Calorimeter clusters associated with charged tracks were also included after the expected calorimeter energy for the associated track is subtracted from the cluster energy to reduce double counting [30]. If the energy of a cluster was smaller than the expected energy for the associated tracks, the cluster energy is not used.

The agreement of the quantity $E_{\text{miss}}^{\text{hemi}}$ between data and Monte Carlo events containing identified leptons following a preselection with relaxed p and p_t cuts to enhance statistics is shown in Fig. 2(a). To further test and calibrate the measurement of this important quantity, event samples from both data and Monte Carlo simulation were prepared that were enhanced in b quarks using a lifetime tag in one hemisphere. Hemispheres were identified as containing b hadrons by reconstructing secondary vertices and using the parameters of the vertices in an artificial neural network trained to reject non-b background [31]. The most important inputs to the neural network were the decay length in the x - y plane, its uncertainty, and the number of tracks in the vertex. The selected sample had a b-quark purity of approximately 90%.

Two control samples were used: one with an electron or muon candidate identified as previously described in the hemisphere opposite the b-tagged hemisphere and another with no lepton identified in the hemisphere opposite the b-tagged hemisphere. The first sample is enriched in energetic neutrinos while the second sample is depleted. From the distributions of the measured and true value of $E_{\text{miss}}^{\text{hemi}}$ in these Monte Carlo samples, small residual neutrino energy shifts were observed. These could be approximated well with an additional average linear correction, determined from both control samples, subtracted from the reconstructed value of $E_{\text{miss}}^{\text{hemi}}$ that ranged from 50 MeV for $E_{\nu}^{\text{true}} = 0$ GeV (i.e., no neutrino) to 910 MeV for $E_{\nu}^{\text{true}} = 30$ GeV. This correction was applied to both the data and Monte Carlo samples to eliminate the small bias inherent in the neutrino energy reconstruction method. The agreement between data and Monte Carlo simulated events in these control samples can be seen in Fig. 2(b) and (c). Independent samples of events with hemispheres failing the b-tag requirement, both with and without identified leptons, also show good agreement between data and Monte Carlo.

The absolute resolution on the missing energy and hence the neutrino energy improves with increasing neutrino energy from $\sigma(E_{\nu}) = 5.0$ GeV at $E_{\nu} = 0$ GeV to 2.9 GeV at $E_{\nu} = 15$ GeV. In the signal Monte Carlo samples, the average neutrino energy resolution was observed to be 3.5 GeV as shown in Fig. 2(d). The average neutrino energy for the unpolarized signal process is about 6.1 GeV with an r.m.s. spread of 4.4 GeV after applying only kinematic and geometric requirements but not including detector resolution effects.

For the electron and muon candidates the momentum was used as an estimate of the lepton energy. For high energy electrons, the electromagnetic cluster energy associated with the electron may have better resolution, but the momentum was used to avoid biases due to overlapping energy deposits of nearby particles. Changes in the electron spectrum due to final-state radiation are included in the Monte Carlo simulation. The distributions of lepton spectra in the control samples described above were also compared between data and Monte Carlo. The shapes agree well and the average values are $\langle E_{\ell} \rangle = 10.18 \pm 0.03$ GeV for the data and $\langle E_{\ell} \rangle = 10.11 \pm 0.03$ GeV for the Monte Carlo simulation for the b-tagged sample containing identified leptons.

The distributions of the measured electron and muon energies and of the reconstructed neutrino energies for the selected right-sign $\Lambda \ell^{-} \pi^{+}$ and wrong-sign $\Lambda \ell^{+} \pi^{+}$ samples in the data are shown in Fig. 3.

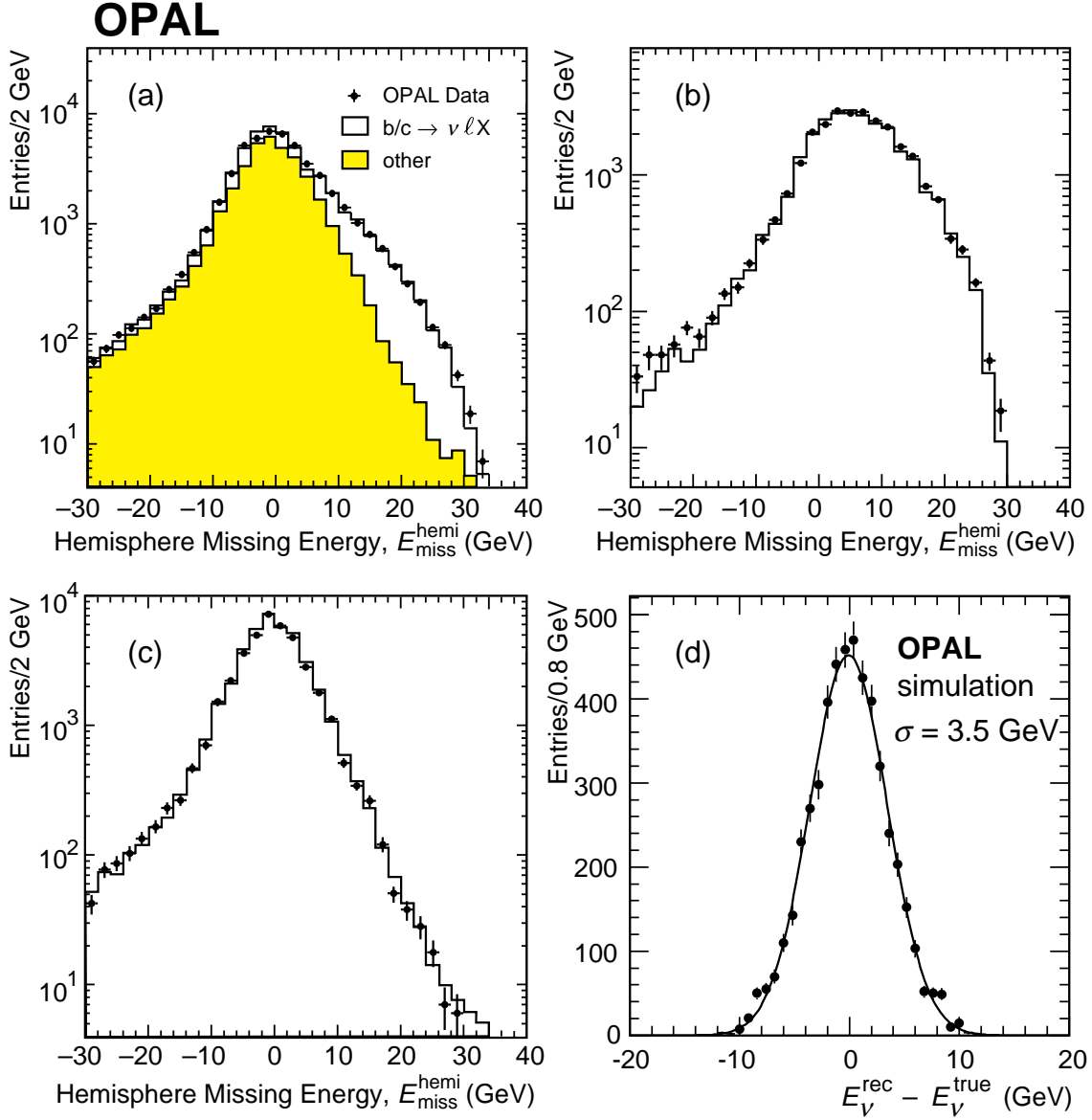


Figure 2: (a) Reconstructed missing energy in data (points with error bars) and Monte Carlo simulated events in $q\bar{q}$ events after a preselection with relaxed p and p_t requirements; the open histogram shows the missing energy for events containing b and c hadrons decaying semileptonically, and the shaded histogram is for all other processes. Reconstructed missing energy for tagged $b\bar{b}$ events in data (points with error bars) and Monte Carlo simulated events (open histograms) (b) with an identified lepton in the hemisphere opposite the b -tag and (c) with no identified lepton in the hemisphere opposite the b -tag. (d) Neutrino energy resolution from reconstructed E_V^{rec} and true E_V^{true} in Monte Carlo signal events with $\Lambda_b^0 \rightarrow \Lambda_c^+ \ell^- \bar{\nu}_\ell X$.

6 Background estimate

The wrong-sign sample is used as an estimate of the level and shape of the background in the right-sign sample. The component of the background due to random combinations of tracks and fakes due to

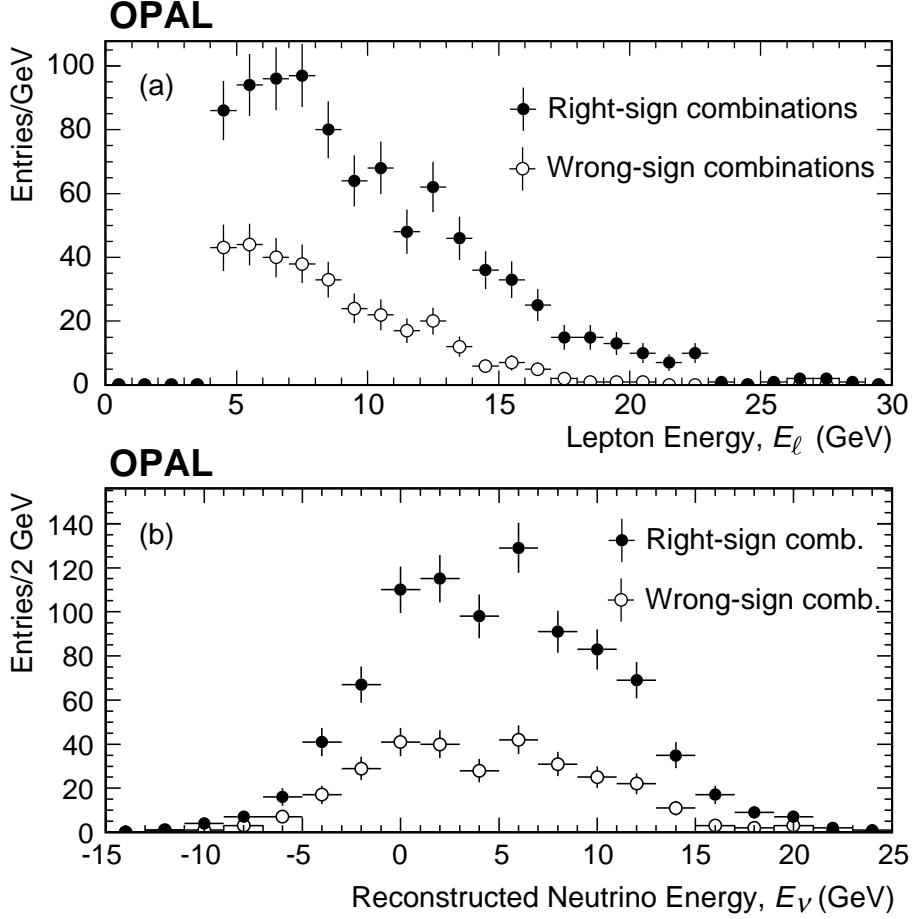


Figure 3: (a) Lepton (electron and muon) and (b) reconstructed neutrino energy spectra for the hemispheres containing selected right-sign $\Lambda_c^- \pi^+$ combinations with the spectra for wrong-sign combinations overlaid.

misidentified leptons or Λ baryons is expected to contribute equally to right- and wrong-sign samples, as verified by Monte Carlo simulations.

A larger source of background is the combination of a Λ baryon from the fragmentation process with a genuine lepton from the semileptonic decay of b or c hadrons. In the framework of string fragmentation, there is a strong correlation between, for example, the Λ_b subsequently decaying as $\Lambda_b \rightarrow \Lambda_c^+ \ell^- \bar{\nu}_\ell X$ and a high momentum $\bar{\Lambda}$ as one of the neighbouring particles in the fragmentation chain. In this case, the background of a fragmentation $\bar{\Lambda} \ell^-$ combination will preferentially enter the wrong-sign sample. Table 1 gives the background composition of the right- and wrong-sign sample as predicted by Monte Carlo simulation and shows the resulting imbalances. These predictions use the “popcorn” model [32] and the indicated uncertainties include modelling effects as described in detail in Ref. [14]. Note that even if a true lepton from a semileptonic Λ_b decay is combined with a fragmentation Λ , the ratio E_ν/E_ℓ is still indicative of b-baryon polarization since missing energy and hence the neutrino energy is calculated using event quantities. Events of this type are therefore treated as signal in the fitting procedure (see below).

A number of exclusive channels as described below are expected to contribute to the right-sign and

Source	RS	WS
Signal: Λ and ℓ from b baryon	629 ± 30	
Fragmentation Λ plus:		
ℓ from B meson	94 ± 9	77 ± 8
ℓ from c baryon	9 ± 3	3 ± 2
ℓ from b baryon	5 ± 4	66 ± 6
ℓ from c meson	32 ± 6	43 ± 7
Exclusive Backgrounds:	32 ± 7	27 ± 6
Combinatorials and Fakes:	111 ± 8	100 ± 8

Table 1: Monte Carlo predictions of the composition among the 912 right-sign (RS) combinations and the 316 wrong-sign combinations. Errors are due to Monte Carlo statistics, branching ratio uncertainties, and modelling systematic errors (see Ref. [14]).

wrong-sign samples, but the total contributions are predicted to be small compared to the background due to combinatorials and fakes and fragmentation Λ baryons. For example, a b baryon can decay semileptonically into a τ lepton that subsequently decays into an electron and muon to enter into the right-sign sample as background. The τ polarization in this case was varied within its range of uncertainties [22] allowing the Λ_b polarization to vary between 0 and -1 to estimate the systematic error on the Monte Carlo prediction for this rate. The expected contribution to the wrong-sign sample for leptons arising from the process $\Lambda_c^+ \rightarrow \Lambda \ell^+ \nu_\ell$ is kept small by the cut on the $\Lambda \ell$ invariant mass. The uncertainty in this rate can be affected by uncertainties in the polarization of the Λ_c which is varied by reweighting Monte Carlo simulated events as described in Section 9. Other exclusive backgrounds include small fractions of $\Lambda_b \rightarrow \Lambda_c^+ D_s^-$ followed by $D_s^- \rightarrow \ell^- X$ and $\bar{B} \rightarrow Y_c \bar{N} \ell \bar{\nu}$, (where Y_c denotes any c baryon) [14].

7 Fitting procedure

The b-baryon polarization was extracted by comparing the reconstructed distribution of E_ν/E_ℓ in the data to spectra estimated from fully simulated Monte Carlo events corresponding to various values of $\langle P_L^{\Lambda_b} \rangle$ and satisfying all the selection criteria. A binned maximum likelihood fit was used to extract $\langle P_L^{\Lambda_b} \rangle$ by determining which Monte Carlo spectrum gives the best description of the data. To obtain the Monte Carlo spectrum for arbitrary values of $\langle P_L^{\Lambda_b} \rangle$, polynomial fits are made bin by bin as a function of $\langle P_L^{\Lambda_b} \rangle$ to allow interpolation between spectra. The binned likelihood method has several advantages over analytical functions used to describe the data distributions and resolutions in an unbinned likelihood fit: it takes into account correlations between E_ν , E_ℓ , $\sigma(E_\nu)$ and $\sigma(E_\ell)$; effects of kinematic cuts such as the minimum lepton energy; energy, momentum, and missing energy resolution with a full simulation of the detector response; and any variation of the selection efficiency with E_ν/E_ℓ .

The probability density function (PDF) was estimated by the binned and normalized Monte Carlo spectrum with $\mathcal{P}_i^{\text{sig}}(P_L^{\Lambda_b})$ being the value of the PDF in bin i of 30 bins for the predicted signal distribution for the average polarization value $\langle P_L^{\Lambda_b} \rangle$. $\mathcal{P}_i^{\text{back}}$ is the normalized Monte Carlo spectrum of the wrong-sign backgrounds listed in Table 1 excluding the contribution of a fragmentation Λ combined with a genuine lepton from a b-baryon decay. The expected number of entries in bin i of

the right-sign and wrong-sign distributions are n_i^{RS} and n_i^{WS} given by:

$$\begin{aligned} n_i^{\text{WS}} &= \mathcal{P}_i^{\text{WS}}(P_L^{\Lambda_b}) \cdot N_{\text{tot}}^{\text{WS}} \\ n_i^{\text{RS}} &= \left[(1 - f^{\text{WS}}) \mathcal{P}_i^{\text{sig}}(P_L^{\Lambda_b}) + f^{\text{WS}} \mathcal{P}_i^{\text{WS}}(P_L^{\Lambda_b}) \right] \cdot N_{\text{tot}}^{\text{RS}}, \\ \text{with } \mathcal{P}_i^{\text{WS}}(P_L^{\Lambda_b}) &= (1 - f_{\text{sig}}^{\text{WS}}) \mathcal{P}_i^{\text{back}} + f_{\text{sig}}^{\text{WS}} \mathcal{P}_i^{\text{sig}}(P_L^{\Lambda_b}). \end{aligned}$$

Here $f_{\text{sig}}^{\text{WS}}$ is the estimated fraction of fragmentation Λ combined with leptons from b baryon decays as given in Table 1, $N_{\text{tot}}^{\text{RS}}$ and $N_{\text{tot}}^{\text{WS}}$ are the total number of right-sign and wrong-sign combinations observed in the data, and $f^{\text{WS}} = N_{\text{tot}}^{\text{WS}}/N_{\text{tot}}^{\text{RS}}$.

The binned likelihood \mathcal{L} is the product of Poisson probabilities for obtaining the numbers of events observed in the data in each bin using the Monte Carlo expectation in that bin for a given $\langle P_L^{\Lambda_b} \rangle$ for both the wrong-sign and right-sign spectra. A normalization constraint was imposed on the total number of observed right-sign combinations. An adjusted likelihood [33] was used to take into account statistical fluctuations in the Monte Carlo prediction. The above assumes that both the level and shape of the wrong-sign sample can be used to estimate the background in the right-sign sample. After removing the signal component in the Monte Carlo wrong-sign combinations, the distribution of E_ν/E_ℓ is consistent with the distribution of the background in the right-sign Monte Carlo combinations. Effects of differences are addressed as systematic errors below.

Further checks of the fitting procedure were performed using Monte Carlo samples. Fully simulated Monte Carlo subsamples of known $\langle P_L^{\Lambda_b} \rangle$, each corresponding to the same number of combinations observed in the data were used as input to the fit and no bias was observed at the precision studied. A simple Monte Carlo program was used to generate an ensemble of 2000 samples, each with the same statistics as selected in the data. For a given value of $\langle P_L^{\Lambda_b} \rangle$, lepton and neutrino energies were randomly sampled from analytical joint energy distributions, smeared according to parameterized energy resolution functions, and kinematic cuts applied. The background and distribution was generated assuming zero polarization and the wrong-sign distribution sampled separately, including a signal component as expected in the data. In all cases, no significant additional systematic biases were observed, and residuals divided by the error on $\langle P_L^{\Lambda_b} \rangle$ indicated a correct evaluation of statistical errors by the likelihood fit. Lastly, the complete analysis was applied directly to the approximately 4 million fully simulated hadronic Monte Carlo events. The fitted value of $\langle P_L^{\Lambda_b} \rangle = -0.09_{-0.13}^{+0.17}$ is consistent with a value of zero polarization for b baryons as simulated in the Monte Carlo sample.

8 Fit result

The event-by-event distribution of E_ν/E_ℓ was formed, as shown in Fig. 4(a), and the right-sign and wrong-sign distributions were fitted using the described procedure. The resulting curve of $-\log \mathcal{L}$ versus $\langle P_L^{\Lambda_b} \rangle$, offset so the maximum value of $\log \mathcal{L}$ is zero, is shown in Fig. 4(b) indicating a measurement of

$$\langle P_L^{\Lambda_b} \rangle = -0.56_{-0.13}^{+0.20},$$

and a value of zero polarization ruled out at the 95% confidence level (CL), considering only the statistical errors. The χ^2 per degree of freedom is 0.91.

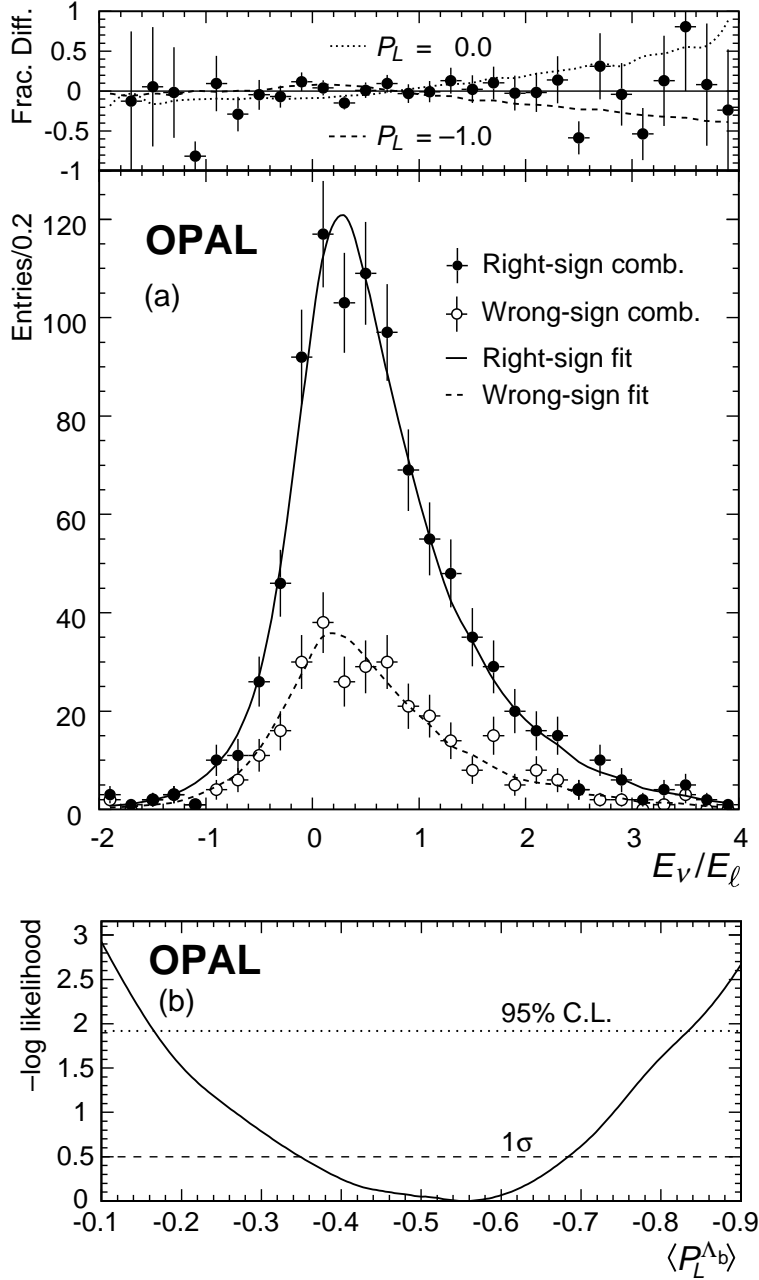


Figure 4: (a) Bottom: distribution of the reconstructed neutrino energy E_ν divided by the electron or muon energy E_ℓ for each right-sign $\Lambda \ell^- \pi^+$ combination in the data (solid circles) overlaid by the distribution for each of the wrong-sign combinations (open circles). The solid and dashed lines show the result of the likelihood fit to the right-sign and wrong-sign distribution, respectively. Top: fractional difference $(n_i^{\text{RS,data}} - n_i^{\text{RS,fit}})/n_i^{\text{RS,fit}}$ (points with error bars) compared to the analogous distributions for the prediction for $\langle P_L^{\Lambda b} \rangle = 0.0$ (dotted line) and $\langle P_L^{\Lambda b} \rangle = -1.0$ (dashed line). (b) Negative log likelihood as a function of $\langle P_L^{\Lambda b} \rangle$ for the fit. The dashed and dotted lines indicate the likelihood change required for one standard deviation errors and 95% CL limits, respectively (statistical errors only).

9 Systematic uncertainties and consistency checks

The sources of systematic error that have been considered are summarized in Table 2.

Source of Uncertainty	$\Delta\langle P_L^{\Lambda_b} \rangle$
E_ν resolution	± 0.02
E_ν reconstruction	± 0.05
E_ℓ scale and shape	± 0.03
Selection criteria	± 0.02
Background fraction and shape	± 0.04
b fragmentation	± 0.03
Λ_c polarization	± 0.02
$b \rightarrow \tau$	± 0.01
Fitting method	± 0.03
Theoretical uncertainty (form factor modelling, QCD corrections, m_c/m_b)	± 0.03
Total	± 0.09

Table 2: *Summary of systematic uncertainties in the measurement of $\langle P_L^{\Lambda_b} \rangle$.*

The overall rate or efficiency for tagging $\Lambda\ell\pi^+$ combinations is not used in the fit but any discrepancy in rate between data and Monte Carlo prediction or distortions as a function of E_ν , E_ℓ , or their ratio can potentially affect the result. Control samples were used in the following to estimate these effects.

To test the Monte Carlo modelling of reconstructed neutrino energy resolution, events with missing energy in the b-tagged Monte Carlo control samples with identified leptons in the range corresponding to the missing energy in the $\Lambda_b \rightarrow \Lambda_c\ell\nu_\ell$ signal were studied. Comparing the resolution $\sigma(E_\nu)$ between the signal sample and the control sample in bins of E_ν , differences of up to 12% were observed. Propagating this resolution uncertainty into the PDF's for E_ν/E_ℓ resulted in differences of ± 0.02 in $\langle P_L^{\Lambda_b} \rangle$.

The linear correction to $E_{\text{miss}}^{\text{hemi}}$ used to reconstruct E_ν was varied within its uncertainties in slope and intercept resulting in an observed variation of ± 0.03 in $\langle P_L^{\Lambda_b} \rangle$. Events with a lepton opposite a hemisphere failing a b-tag were used as an independent data control sample. In this sample, the data and Monte Carlo distributions were normalized to the same number of events and the ratio of the resulting $E_{\text{miss}}^{\text{hemi}}$ distributions in bins of $E_{\text{miss}}^{\text{hemi}}$ was fitted to a first-order polynomial. The fitted slope was consistent with zero, but $\Lambda\ell\pi^+$ combinations were reweighted according to the one standard deviation bounds on a possible slope. It was checked that a fit to a second-order polynomial resulted in no significant parabolic coefficient. Similar results were observed with a sample consisting of events with a lepton opposite a hemisphere passing the b-tag. Variations ranged up to ± 210 MeV in the average value of E_ν and resulted in a change of ± 0.05 in $\langle P_L^{\Lambda_b} \rangle$. This is assigned as the systematic error due to uncertainties in the E_ν reconstruction and its distribution.

The absolute scale of the momentum measurement of electrons and muons was determined by comparing e^+e^- and $\mu^+\mu^-$ pair and photon conversion data with corresponding Monte Carlo simulation. Lepton momenta in the data were rescaled by the observed uncertainty of $\pm 0.4\%$ resulting in a change in $\langle P_L^{\Lambda_b} \rangle$ of ± 0.01 . Possible mismodelling of the electron identification efficiency as a function of E_ℓ was investigated by comparing the relative rate in multihadronic events of cleanly identified photon

conversions with Monte Carlo predictions as a function of electron energy. Similar studies [27] were done for muons as a function of muon momentum. In both cases, relative variations did not exceed 3%, and Monte Carlo E_ℓ spectra were reweighted according to the observed differences. Refitting resulted in observed changes of ± 0.03 in $\langle P_L^{\Lambda_b} \rangle$. The uncertainty in the momentum resolution results in a negligible effect on the polarization and the total assigned systematic error due to uncertainties in the E_ℓ distributions was ± 0.03 .

The selection criteria were varied within typical ranges of their resolution as determined by signal Monte Carlo samples and the fit repeated. The observed variations of ± 0.02 in $\langle P_L^{\Lambda_b} \rangle$ were assigned as a systematic error.

The effect of uncertainties in the determination of the shape of the wrong-sign background PDF and the level of the background was assessed by varying each component by its uncertainty indicated in Table 1. Since the background due to a fragmentation Λ baryon combined with a lepton from b-baryon decay was predicted to be $(21 \pm 3)\%$ of the wrong-sign sample, the fit was also repeated after scaling down the background in the right-sign sample by this factor. Lastly, instead of using the wrong-sign background PDF fit to the number of wrong-sign combinations, the distribution of E_ν/E_ℓ in the data wrong-sign combinations was simply subtracted from the distribution of the right-sign combinations and the fit to the signal PDF's repeated. The observed changes from the central value of $\langle P_L^{\Lambda_b} \rangle$ in these tests were added in quadrature resulting in a systematic error of ± 0.04 assigned due to uncertainties in the background estimate.

The fragmentation parameter $\langle x_E \rangle_b$, defined as the average fraction of the beam energy carried by a weakly decaying b hadron, has been estimated to be the same for baryons and mesons at the 1% level [11]. Varying the average Λ_b energy by the measured errors on the average b-hadron energy [34] added in quadrature with this 1% uncertainty results in a variation of $\langle P_L^{\Lambda_b} \rangle$ of ± 0.03 due to the residual logarithmic dependence on fragmentation of the E_ν/E_ℓ distribution [12].

Polarization of the Λ_c^+ baryon can affect the acceptance for combinations in the signal chain $\Lambda_b \rightarrow \Lambda_c^+ \ell^- \bar{\nu}_\ell$, $\Lambda_c^+ \rightarrow \Lambda X$, $\Lambda \rightarrow p\pi^-$ and also the lepton spectra from background semileptonic decays of Λ_c either produced in the above chain or via direct production in $Z^0 \rightarrow c\bar{c}$ events. In the first two cases, measured Λ_c decay parameters [19] were used and $\Lambda\ell\pi^+$ Monte Carlo combinations involving Λ_c baryons entering the sample for the background PDF were reweighted (also see Ref. [35]) to correspond to variations of the Λ_c polarization between 0 and -1 . In the latter case, the Λ_c polarization was varied between 0 and -0.68 , the value for c quarks produced in $Z^0 \rightarrow c\bar{c}$. The fitted value of $\langle P_L^{\Lambda_b} \rangle$ changed by ± 0.02 , which is assigned as a systematic error due to this effect.

The measured branching ratio for $\text{Br}(b \rightarrow \tau \bar{\nu}_\tau X)$ was varied within its uncertainties [36] and the level of transfer of polarization of the tau chosen from an alternative model [22] to reweight Monte Carlo background combinations. The effect was small, and a systematic error of ± 0.01 due to this background source uncertainty was assigned.

Monte Carlo tests for possible biases in the fitting method have already been described earlier. In addition, the binning of the spectra and the PDF's was varied from 30 bins to 20 and 40 bins. The range of the fit was also changed from $-2 \leq E_\nu/E_\ell \leq 4$ to $-1 \leq E_\nu/E_\ell \leq 3$ and the fit repeated. Adding the observed variations in $\langle P_L^{\Lambda_b} \rangle$ in quadrature, a systematic error of ± 0.03 was assigned due to possible biases introduced by the fitting method.

Many sources of uncertainty in the lepton and neutrino energy spectra partially cancel in the ratio E_ν/E_ℓ . For the input to the theoretical calculation of these spectra for polarized b baryons including

QCD corrections [10], the ratio m_c/m_b was varied in the range 0.22–0.39 and the strong coupling constant $\alpha_S(m_b)$ in the range 0.20–0.24 [19]. An alternative simple quark model [37] using different form factors in the polarized Λ_b^0 decay was also substituted. The signal Monte Carlo spectra were weighted accordingly. Different masses of b baryons and c baryon decay products (e.g., Ξ_b and Ξ_c) were also used in the calculation of the spectra. In all cases the fit was repeated and from the observed variation in $\langle P_L^{\Lambda_b} \rangle$, a systematic error of ± 0.03 was assigned due to theoretical uncertainties in the predicted E_ν/E_ℓ spectra.

The systematic uncertainties from each source were added in quadrature to obtain an estimated total systematic error of ± 0.09 on $\langle P_L^{\Lambda_b} \rangle$.

Consistency Checks: Further checks were performed to search for other systematic effects. The cut on the minimum momentum of the electron or muon was varied between 3.0 and 5.0 GeV, and the requirement on the minimum p_t changed between 0.6 and 1.0 GeV. These variations change the b quark content of the sample; in particular the Λ_c and charm meson content increases for the smaller p_t cut. The minimum momentum of the Λ candidate was varied in the range 3.0 to 5.0 GeV, increasing and decreasing the background level of fragmentation Λ baryons being combined with leptons. In each case the analysis was repeated and $\langle P_L^{\Lambda_b} \rangle$ redetermined. Observed variations were consistent with the statistical errors on the uncorrelated fractions of the different samples.

The fit was performed separately for data collected in 1990–1993 and for 1994–1995, and also separately for $\Lambda e^- \pi^+$ and $\Lambda \mu^- \pi^+$ combinations. All results were statistically consistent with each other and with the central value from the full data set. The observed rate of $\Lambda \ell^- \pi^+$ combinations were also consistent in these different samples, and the derived value $f(b \rightarrow \Lambda_b) \cdot \text{Br}(\Lambda_b \rightarrow \Lambda \ell \bar{\nu}_\ell X) = (2.78 \pm 0.16) \times 10^{-3}$ (statistical error only) agrees with previous OPAL measurements [14, 38] within errors.

A fit was also made to the reconstructed E_ν/E_ℓ distribution in the inclusive lepton control sample from the data. This large statistics sample consisted of events with an identified lepton in the hemisphere opposite to a b-tagged hemisphere. No wrong-sign background subtraction was performed, and a longitudinal polarization of $\langle P_L \rangle = -0.043 \pm 0.019$ (stat.) was measured. Although B mesons are expected to be unpolarized (the ground states are unpolarized and for spin-1 states the polarization is undetectable), a fraction $(10.1_{-3.1}^{+3.9})\%$ [19] of the b hadrons are predicted to be b baryons in this sample, and there will also be a contamination of polarized c baryons that decay weakly. In addition, the smaller expected semileptonic branching ratio for b baryons compared to the other b hadrons [38, 19] would result in further reduction of total observed polarization. Although the total observed polarization is not necessarily expected to be zero, it should be small, as observed.

A further cross check was made with a data sample containing candidates for the exclusive decay $B^0 \rightarrow D^{*-} \ell^+ \nu_\ell$ selected from events where a D^{*-} and a lepton of opposite charge were found in the same jet [39]. A value consistent with zero, $\langle P_L \rangle = 0.07_{-0.12}^{+0.13}$, was found as expected for a sample with a b hadron content almost exclusively from B mesons and much less contamination from possibly polarized heavy baryons.

10 Discussion and summary

The average polarization of b baryons in Z^0 decays at OPAL has been measured to be:

$$\langle P_L^{\Lambda_b} \rangle = -0.56_{-0.13}^{+0.20} \pm 0.09,$$

where the first error is statistical and the second systematic. This level of polarization is larger than, but consistent with, the published measurement by the ALEPH Collaboration [40] of $\langle P_L^{\Lambda_b} \rangle = -0.23_{-0.20}^{+0.24}$ (stat.) $_{-0.07}^{+0.08}$ (syst.).

Including systematic errors, this OPAL measurement implies bounds on the longitudinal polarization of b baryons of $-0.13 \geq \langle P_L^{\Lambda_b} \rangle \geq -0.87$ at 95% CL, therefore disfavoring full observed average polarization of -0.94 . This is the first measurement to exclude zero polarization of b baryons at larger than 95% CL providing direct evidence that the b quark is longitudinally polarized in the decay $Z^0 \rightarrow b\bar{b}$.

A simple model [4] can be used to predict the total observed b baryon polarization after depolarization of those b baryons proceeding through intermediate states involving strong decays: $b \rightarrow \Sigma_b^{(*)} \rightarrow \Lambda_b$. The prediction depends on a parameter A that is the relative probability of producing a spin $S = 1$ diquark as opposed to a $S = 0$ diquark, and a parameter ω_1 that is the probability that the spin 1 diquark has angular momentum component $j_3 = \pm 1$ along the fragmentation axis. For $\omega_1 = 0$ (alignment suppression) and the default JETSET parameter⁴ for A , a value of $\langle P_L^{\Lambda_b} \rangle = -0.68$ is predicted. Varying ω_1 to 0.66 (isotropic diquark spin distribution) and A within bounds suggested by measurements [41] gives a range of predictions between -0.54 and -0.88 . In this model, the measured value of $\langle P_L^{\Lambda_b} \rangle$ is consistent with no depolarization during fragmentation. It is also consistent with the inclusive Λ measurement of OPAL [42] that also found no evidence of polarization loss in hadronization.

Acknowledgements

We thank M. Jezabek for providing the FORTRAN program of the calculations of the neutrino and lepton spectra as described in Ref. [10]. We particularly wish to thank the SL Division for the efficient operation of the LEP accelerator at all energies and for their continuing close cooperation with our experimental group. We thank our colleagues from CEA, DAPNIA/SPP, CE-Saclay for their efforts over the years on the time-of-flight and trigger systems which we continue to use. In addition to the support staff at our own institutions we are pleased to acknowledge the

Department of Energy, USA,

National Science Foundation, USA,

Particle Physics and Astronomy Research Council, UK,

Natural Sciences and Engineering Research Council, Canada,

Israel Science Foundation, administered by the Israel Academy of Science and Humanities,

Minerva Gesellschaft,

Benozio Center for High Energy Physics,

Japanese Ministry of Education, Science and Culture (the Monbusho) and a grant under the Monbusho International Science Research Program,

German Israeli Bi-national Science Foundation (GIF),

Bundesministerium für Bildung, Wissenschaft, Forschung und Technologie, Germany,

National Research Council of Canada,

Research Corporation, USA,

Hungarian Foundation for Scientific Research, OTKA T-016660, T023793 and OTKA F-023259.

⁴In the JETSET package, $A \approx 9 \cdot \text{PAR}(4)$.

References

- [1] F.E. Close, J.G. Körner, R.J.N. Phillips, and D.J. Summers, *J. Phys.* **G18** (1992) 1716.
- [2] T. Mannel and G. Schuler, *Phys. Lett.* **B279** (1992) 194.
- [3] J.G. Körner, A. Pilaftsis, and M. Tung, *Z. Phys.* **C63** (1994) 575;
M. Tung, *Phys. Rev.* **D52** (1995) 1353;
S. Groote, J.G. Körner, and M. Tung, *Z. Phys.* **C74** (1997) 615.
- [4] A.F. Falk and M.E. Peskin, *Phys. Rev.* **D49** (1994) 3320.
- [5] J. Körner, *Nucl. Phys. B, Proc. Suppl.* **50** (1996) 130.
- [6] J.F. Amundson, J.L. Rosner, M. Worah, and M.B. Wise, *Phys. Rev.* **D47** (1993) 1260;
M. Gronau, in *B Decays*, 2nd Edition, ed. by S. Stone, World Scientific (1994).
- [7] J.H. Field, *A Model Independent Analysis of LEP and SLD Data Z Decays: Is the Standard Model Confirmed?*, UGVA-DPNC 1997/10-172 Oct. 1997, submitted to *Phys. Rev. D*;
T. Rizzo, *Right-Handed Currents in B Decay Revisited*, SLAC-PUB-7738, March 1998, submitted to *Phys. Rev. D*.
- [8] B. Mele and G. Altarelli, *Phys. Lett.* **B299** (1993) 345;
B. Mele, *Mod. Phys. Lett.* **A9** (1994) 1239.
- [9] I.I. Bigi, M. Shifman, N.G. Uraltsev, and A. Vainshtein, *Phys. Rev. Lett.* **71** (1993) 496;
A. Czarnecki, M. Jezabek, J.G. Körner, and J.H. Kühn, *Phys. Rev. Lett.* **73** (1994) 384.
- [10] A. Czarnecki and M. Jezabek, *Nucl. Phys.* **B427** (1994) 3.
- [11] G. Bonvicini and L. Randall, *Phys. Rev. Lett.* **73** (1994) 392.
- [12] C. Diaconu, M. Talby, J.G. Körner, and D. Pirjol, *Phys. Rev.* **D53** (1996) 6186.
- [13] OPAL Collab., P.D. Acton *et al.*, *Phys. Lett.* **B281** (1992) 394.
- [14] OPAL Collab., R. Akers *et al.*, *Z. Phys.* **C69** (1996) 195.
- [15] ALEPH Collab., D. Buskulic *et al.*, *Phys. Lett.* **B365** (1996) 437.
- [16] OPAL Collab., K. Ahmet *et al.*, *Nucl. Inst. Meth.* **A305** (1991) 275;
P.P. Allport *et al.*, *Nucl. Inst. Meth.* **A346** (1994) 476;
P.P. Allport *et al.*, *Nucl. Inst. Meth.* **A324** (1993) 34.
- [17] O. Biebel *et al.*, *Nucl. Inst. Meth.* **A323** (1992) 169;
M. Hauschild *et al.*, *Nucl. Inst. Meth.* **A314** (1992) 74.
- [18] B.E. Anderson *et al.*, *IEEE Transactions on Nuclear Science* **41** (1994) 845.
- [19] Particle Data Group, C. Caso *et al.*, *Eur. Phys. J.* **C3** (1998) 1.
- [20] JETSET 7.404a and 7.408 generator: T. Sjöstrand, *Comp. Phys. Comm.* **82** (1994) 74;
T. Sjöstrand, LUTP 95-20.
The OPAL parameter optimization is described in
OPAL Collab., G. Alexander *et al.*, *Z. Phys.* **C69** (1996) 543.

- [21] C. Peterson *et al.*, *Phys. Rev.* **D27** (1983) 105.
- [22] A. Falk, Z. Ligeti, M. Neubert, and Y. Nir, *Phys. Lett.* **B326** (1994) 145;
M. Gremm, G. Köpp, and L.M. Sehgal, *Phys. Rev.* **D52** (1995) 1588.
Also see S. Balk, J.G. Korner, and D. Pirjol, *Eur. Phys. J.* **C1** 221.
- [23] S. Jadach, Z. Was, R. Decker, and J.H. Kühn, *Comp. Phys. Comm.* **76** (1993) 361.
- [24] J. Allison *et al.*, *Nucl. Inst. Meth.* **A317** (1992) 47.
- [25] OPAL Collab., G. Alexander *et al.*, *Z. Phys.* **C52** (1991) 175.
- [26] OPAL Collab., R. Akers *et al.*, *Z. Phys.* **C70** (1996) 357.
- [27] OPAL Collab., P.D. Acton *et al.*, *Z. Phys.* **C58** (1993) 523.
- [28] OPAL Collab., R. Akers *et al.*, *Z. Phys.* **C63** (1994) 197.
- [29] JADE Collab., W. Bartel *et al.*, *Z. Phys.* **C33** (1986) 23;
JADE Collab., S. Bethke *et al.*, *Phys. Lett.* **B213** (1988) 235.
- [30] OPAL Collab., K. Ackerstaff *et al.*, *Eur. Phys. J.* **C2** (1998) 213.
- [31] OPAL Collab., R. Akers *et al.*, *Z. Phys.* **C65** (1995) 17.
- [32] B. Andersson, G. Gustafson, and T. Sjöstrand, *Physica Scripta* **32** (1985) 574.
A popcorn model has been implemented in JETSET, where the frequency for the process baryon-meson-antibaryon is regulated in JETSET by the parameter PARJ(5) (with default value 0.5), such that the probability is given by PARJ(5)/(0.5 + PARJ(5)).
- [33] R. Barlow and C. Beeston, *Comp. Phys. Comm.* **77** (1993) 219.
- [34] LEP Experiments: ALEPH, DELPHI, L3, OPAL, *Nucl. Inst. Meth.* **A378** (1996) 101.
- [35] J.-P. Lee, C. Liu, and H.S. Song, *Analysis of $\Lambda_b \rightarrow \Lambda_c$ weak decays in Heavy Quark Effective Theory*, SNUTP-97-099, Mar 1998, to be published in *Phys. Rev. D*.
- [36] ALEPH Collab., D. Buskulic *et al.*, *Phys. Lett.* **B343** (1994) 201;
L3 Collab., M. Acciarri *et al.*, *Phys. Lett.* **B332** (1993) 34.
- [37] B. Holdom, M. Sutherland, and J. Mureika, *Phys. Rev.* **D49** (1994) 2359.
- [38] OPAL Collab., K. Ackerstaff *et al.*, *Z. Phys.* **C74** (1997) 423.
- [39] OPAL Collab., K. Ackerstaff *et al.*, *Phys. Lett.* **B395** (1997) 128.
- [40] ALEPH Collab., D. Buskulic *et al.*, *Phys. Lett.* **B365** (1996) 437.
- [41] OPAL Collab., P.D. Acton *et al.*, *Phys. Lett.* **B291** (1992) 503.
- [42] OPAL Collab., K. Ackerstaff *et al.*, *Eur. Phys. J.* **C2** (1998) 49.